The flavonol glycoside icariin promotes bone formation in growing rats by activating the cAMP signaling pathway in primary cilia of osteoblasts

Received for publication, July 31, 2017, and in revised form, October 29, 2017 Published, Papers in Press, October 31, 2017, DOI 10.1074/jbc.M117.809517

Wengui Shi[‡1], **Yuhai Gao**[‡1], **Yuanyuan Wang**[‡], **Jian Zhou**[‡], **Zhenlong Wei**[‡], **Xiaoni Ma**[‡], **Huiping Ma**[§], **Cory J. Xian**[¶2], **Jufang Wang**[‖3], **and Keming Chen**[‡4]

From the [‡]*Institute of Orthopaedics and the* [§]*Department of Pharmacy, Lanzhou General Hospital of CPLA, Lanzhou 730050, China, the* [¶]*Sansom Institute for Health Research, School of Pharmacy and Medical Sciences, University of South Australia, Adelaide, SA 5001, Australia, and the* [‖]*Key Laboratory of Space Radiobiology of Gansu Province, Institute of Modern Physics, Chinese Academy of Sciences, Lanzhou 730000, China*

Edited by Ronald C. Wek

Icariin, a prenylated flavonol glycoside isolated from the herb *Epimedium*, has been considered as a potential alternative therapy for osteoporosis. Previous research has shown that, unlike other flavonoids, icariin is unlikely to act via the estrogen receptor, but its exact mechanism of action is unknown. In this study, using rat calvarial osteoblast culture and rat bone growth models, we demonstrated that icariin promotes bone formation by activating the cAMP/protein kinase A (PKA)/cAMP response element–binding protein (CREB) pathway requiring functional primary cilia of osteoblasts. We found that icariin increases the peak bone mass attained by young rats and promotes the maturation and mineralization of rat calvarial osteoblasts. Icariin activated cAMP/PKA/CREB signaling of the osteoblasts by increasing intracellular cAMP levels and facilitating phosphorylation of both PKA and CREB. Blocking cAMP/PKA/CREB signaling with inhibitors of the cAMP-synthesizing adenylyl cyclase (AC) and PKA inhibitors significantly inhibited the osteogenic effect of icariin in the osteoblasts. Icariin-activated cAMP/PKA/CREB signaling was localized to primary cilia, as indicated by localization of soluble AC and phosphorylated PKA. Furthermore, blocking ciliogenesis via siRNA knockdown of a cilium assembly protein, IFT88, inhibited icariin-induced PKA and CREB phosphorylation and also abolished icariin's osteogenic effect. Finally, several of these outcomes were validated in icariin-treated rats. Together, these results provide new insights into icariin function and its mechanisms of action and strengthen existing ties between cAMP-mediated signaling and osteogenesis.

Icariin is a prenylated flavonol glycoside isolated from a traditional Chinese medicinal herb *Epimedium*, which has long been used to treat bone fractures and prevent osteoporosis (1). We and others have previously reported that icariin can increase osteogenic differentiation and mineralization of bone marrow stromal cells (BMSCs)[5] and osteoblasts, and inhibits osteoclast formation and their bone resorption activity (2–4). Animal experiments indicate that icariin has an anabolic effect, increases bone formation, and suppresses bone loss in ovariectomized rats and osteoprotegerin-deficient mice (5, 6). In addition, a 24-month randomized, double-blind and placebo-controlled trial found that Epimedium-derived flavonoids exerted beneficial effects of preventing bone loss in elderly postmenopausal women without any detectable effect of hyperplasia in the endometrium (7).

The two most significant risk factors associated with the development of osteoporosis are the peak bone mass achieved and the rate of bone loss. Peak bone mass is believed to be achieved before the end of the third decade in life and a low peak bone mass has been considered as a risk factor for developing osteoporosis later in life (8). However, the role of icariin on the augmentation of peak bone mass is still unknown. More importantly, the action mechanism of icariin, especially the initial signaling events induced by icariin remains unclear.

Icariin and other flavonoids have been extensively studied as phytoestrogens and their bone-protecting action is usually considered to result from the direct estrogen receptor (ER)-mediated action on osteoblasts, because of the structure similarity between flavonoids and β-estradiol (9, 10). However, a competitive radioligand binding assay between icariin and ER indicated that icariin had no binding affinity for ERα or ERβ, and an ER-mediated luciferase activity assay showed that icariin could not activate estrogen response element–dependent transcrip-

This work was supported in part by National Natural Sciences Foundation of China Grants 81270963, 81471090, and 81770879, the International Science & Technology Cooperation Program of China Grant 2015DFR30940, Natural Sciences Foundation of Gansu province Grant 1506RJZA307, and the Science and Technology Research Project of Gansu Province Grants 145RTSA012 and 17JR5RA307. The authors declare that they have no conflicts of interest with the contents of this article.

This article contains supplemental Figs. S1–S6.

[1] Both authors contributed equally to the results of this work.

[2] Supported by National Health and Medical Research Council (NHMRC) Australia Senior Research Fellowship number 1042105.

[3] To whom correspondence may be addressed. Tel.: 86-0931-4969164; E-mail: jufangwang@impcas.ac.cn.

[4] To whom correspondence may be addressed. Tel.: 86-0931-8994327; E-mail: chenkm@lut.cn.

[5] The abbreviations used are: BMSC, mineralization of bone marrow stromal cell; ER, estrogen receptor; PTH, parathyroid hormone; AC, adenylyl cyclase; BMD, bone mineral density; DEXA, dual-energy X-ray absorptiometer; BV/TV, trabecular bone volume; Tb.Th, trabecular thickness; Tb.N, trabecular number; Tb.S, trabecular separation; ALP, alkaline phosphatase; DDA, 2′,3′-dideoxyadenosine; PDE4, phosphodiesterase 4; sAC, soluble AC; IFT88, intraflagellar transport 88; tmAC, transmembranous adenylyl cyclases; *p*-PKA, phosphorylated PKA; *p*-CREB, phosphorylated CREB.

tion via ERα or ERβ in a way similar to that of estradiol (11, 12). Furthermore, we have previously shown that icariin is more potent than genistein, a well known phytoestrogen, in promoting osteoblastic differentiation and mineralization, whereas the estrogenic activity of icariin is much weaker than that of genistein (13, 14). Besides, compared with genistein, the molecular structure of icariin was obviously different from β-estradiol because of the existence of a prenyl group on C-8 (15). These studies demonstrated that there may exist a non-phytoestrogenic mechanism for the osteotropic function of icariin, and that the estrogen-dependent mechanism may play a secondary role. Thus searching for the fundamental mechanism for icariin-induced osteogenesis is still ongoing.

Studies have suggested that the cAMP-protein kinase A (PKA) signaling system is responsible for regulating osteogenic differentiation and mineralization, and its activation is required for osteogenic responses to bone formation promoters (16). Indeed parathyroid hormone (PTH) with notable effects on the treatment of osteoporosis was found to stimulate production of cAMP, activation of cAMP-PKA signaling, and the downstream phosphorylation (p) of cAMP response element–binding protein (CREB) to enhance the proliferation, osteogenic differentiation, and mineralization of BMSCs (16–18). In the current work, we hypothesized that icariin stimulates bone formation by activating cAMP-PKA pathway.

Primary cilium is a microtubule structure protruding from the cell surface like a cellular antenna on almost every mammalian cell, and has been reported to be a mechanosensor and chemosensor (19, 20). It was found that primary cilium was essential for cAMP signaling transduction, and multiple components of cAMP-PKA signaling such as G-protein–coupled receptors (Gpr161) and adenylyl cyclase (AC) preferentially localized to the cilium (21–22). It is now known that a variety of receptors, ion channels, and transporter proteins, as well as some of their downstream molecules have been localized to the cilium, and that primary cilium is critical for osteogenic process stimulated by bone formation promoters including fluid flow and electromagnetic fields (23–26). Defects in primary cilium structure or mutations disrupting ciliogenesis will lead to a variety of developmental abnormalities and postnatal disorders (27). Based on these reports, we further hypothesized that icariin stimulated osteogenic differentiation of osteoblasts due to the activation of the cAMP/PKA/CREB pathway, which was mediated through the primary cilium. In the present study, using osteoblast culture and rat bone growth models, we demonstrated that, instead of the estrogen-dependent mechanism, the primary cilium–mediated cAMP/PKA/CREB signaling pathway plays a key role in the osteotropic function of icariin.

Results

Icariin augmented peak bone mass of growing rats

To investigate the effects of icariin on the attainment of peak bone mass in growing rats, the animals were euthanized (at 3 months of age) after 2 months of icariin administration, and the bone mineral density (BMD) (by dual-energy X-ray absorptiometer, DEXA) and bone strength (by biomechanics tests) of isolated femurs and vertebrae were determined, and the bone structure and volume of the tibias and femurs were examined (by bone histomorphometric and microcomputer tomography, micro-CT). The levels of bone formation marker osteocalcin and the activity of bone resorption marker TRACP 5b in the serum were also analyzed. As shown in Fig. 1, *A* and *B*, icariin significantly improved the BMD of femurs ($p < 0.05$) and vertebrae ($p < 0.001$) when compared with the control. Results of biomechanical analyses showed that the icariin group exhibited significantly higher ultimate loads of femurs ($p < 0.001$) and vertebrae ($p < 0.05$) than the control (Fig. 1, *C* and *D*). Biochemical analyses of bone turnover markers showed that icariin dramatically increased the levels of serum osteocalcin ($p < 0.05$) and decreased the activity of TRACP 5b ($p < 0.01$) when compared with the control (Fig. 1, *E* and *F*). Micro-CT analyses of the cancellous bone of distal femur showed that the trabecular BMD (tBMD), trabecular bone volume (BV/TV), trabecular thickness (Tb.Th), and trabecular number (Tb.N) were increased by 15.70 ($p < 0.05$, Fig. 1*G*), 24.96 ($p < 0.05$, Fig. 1*H*), 34.07 ($p < 0.01$, Fig. 1*I*), and 24.51% ($p < 0.05$, Fig. 1*J*), respectively, whereas the trabecular separation (Tb.Sp) was reduced by 42.5% ($p < 0.05$, Fig. 1*K*) in the icariin group when compared with the control. No significant differences were observed for the mid-shaft femur cortical bone between the icariin group and the control (supplemental Fig. S1). Bone histomorphometric analyses for the microarchitecture of tibial metaphysis revealed the same tendency with micro-CT analyses on distal femora (Fig. 1*M*). These results confirmed that icariin treatment promotes attainment of peak bone mass of growing rats. Furthermore, pathological observation of the main organs including liver, kidney, spleen, and uterus found no harmful changes in the icariin-treated group (supplemental Fig. S2).

Osteoblasts responded to icariin with cAMP/PKA/CREB signaling activation

To investigate whether the cAMP/PKA/CREB pathway was involved in the icariin-induced osteoblastic differentiation and maturation, we first screened the optimal concentration of icariin for its osteogenic activity. As shown in Fig. 2, icariin at 10^{-7}, 10^{-6}, and 10^{-5} M significantly promoted the alkaline phosphatase (ALP) activity of rat calvarial osteoblasts after 3 and 6 days (Fig. 2*A*) and increased the number and the areas of mineralized nodules after 12 days (Fig. 2, *B* and *C*). In particular, 10^{-6} M was found to be the optimal concentration that promoted the ALP activity ($p < 0.001$) and augmented the calcified nodule formation at the highest level ($p < 0.001$).

Then we analyzed the changes of the intracellular cAMP level after the osteoblasts were exposed to 10^{-6} M icariin for different time periods. As shown in Fig. 3*A*, the cAMP content increased rapidly and persistently. It began to increase after 5 min, reaching a level significantly higher than the starting point after 10 min ($p < 0.001$), and showing persistently higher levels afterward until 120 min ($p < 0.001$). To examine the possibility that the higher cAMP response would be obtained by different concentrations of icariin, the osteoblasts were treated by icariin from 10^{-4} to 10^{-8} M, respectively. The cAMP level was increased in a dose-dependent manner, and the highest level was obtained at 10^{-4} M (supplemental Fig. S3). Because 10^{-6} M icariin was the optimal concentration for the osteogenic

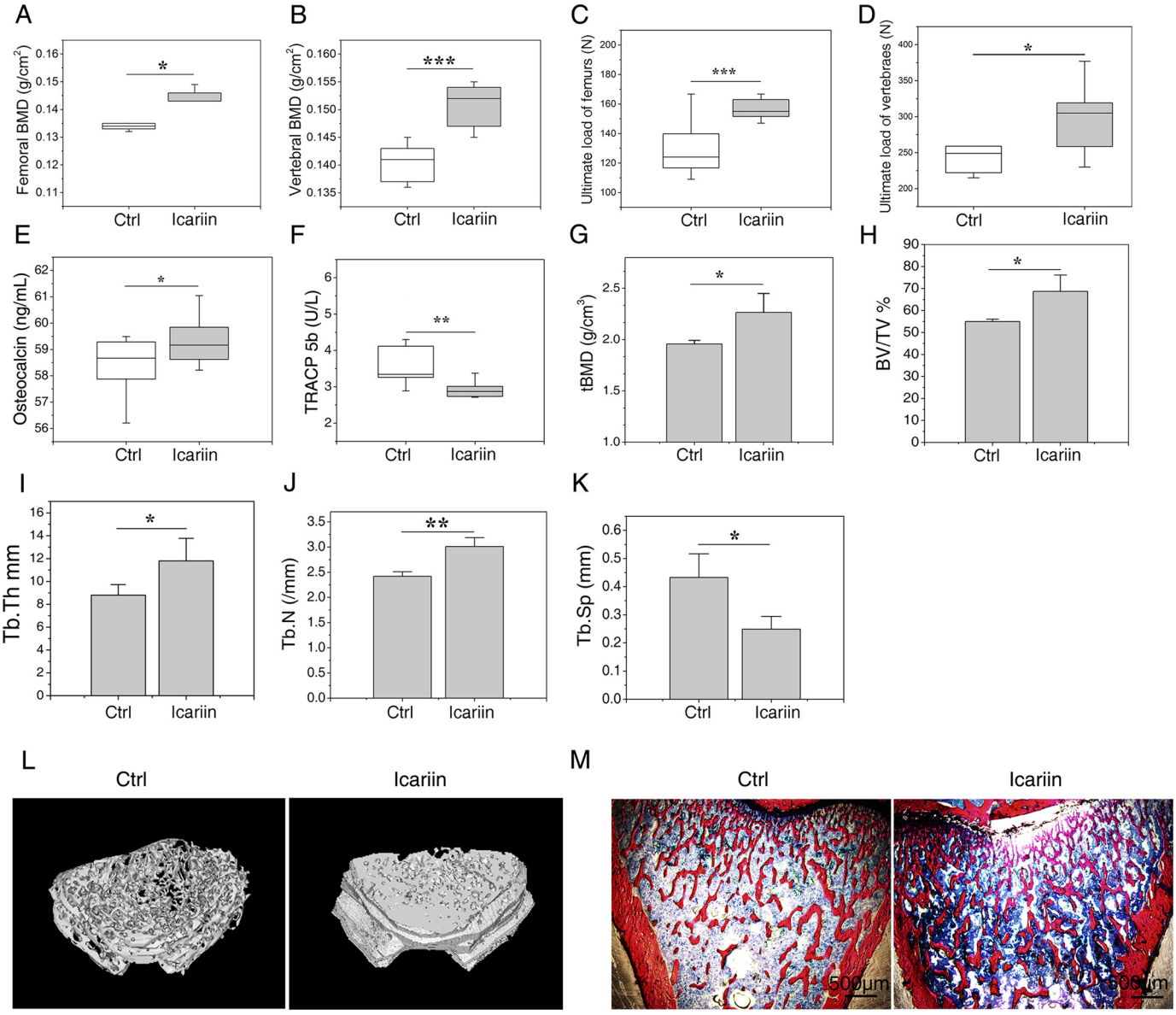

Figure 1. Icariin augmented attainment of peak bone mass in rats. *A* and *B,* BMD of the femurs (*A*) and the vertebrae (*B*) after 2 months of icariin administration. *C* and *D,* biomechanical property analyses results: ultimate load of the femurs obtained by three-point bending tests (*C*), ultimate load of the vertebrae by compression tests (*D*). *E* and *F,* the serum biochemical marker analysis results: the bone formation marker osteocalcin (*E*) and the bone resorption marker TRACP 5b (*F*). *G–K*, the microcomputer tomography (μCT) analyses results for femurs: BMD (mg/cm^3) (*G*), bone volume fraction (BV/TV) (*H*), trabecular thickness (Tb.Th) (*I*), trabecular number (Tb.N) (*J*), and trabecular spacing (Tb.Sp) (*K*). *L,* representative μCT images showing the microarchitectural structure of the trabecular bone of distal femur. *M,* representative images of bone histomorphometric analyses showing the microarchitectural structure of the trabecular bone of proximal tibias. Each experiment was conducted at least three times independently. Data are represented as mean ± S.D. ($n = 8$); *, $p < 0.05$; **, $p < 0.01$; ***, $p < 0.001$ when compared with control (*Ctrl*).

activity, and cAMP content was increased significantly at this concentration, 10^{-6} M icariin was used in the subsequent experiments.

It was found that icariin treatment induced phosphorylation of PKA (*p*-PKA) and CREB (*p*-CREB) after 10 min, and became more obvious with the treatment time, whereas the total PKA and CREB levels remained unchanged (Fig. 3*B*). To further identify the pathway activation, the localization of *p*-PKA was examined by immunofluorescence staining. *p*-PKA was positively localized in the nucleus of osteoblasts after 120 min in the icariin group, whereas no nuclear translocation of *p*-PKA was found in the control (Fig. 3*C*).

Icariin-induced osteogenesis was inhibited after cAMP/PKA/CREB signaling was blocked

To investigate whether icariin stimulates osteogenic differentiation via activating the cAMP/PKA/CREB signaling pathway, the osteoblasts were pretreated with 2′,3′-dideoxyadenosine (DDA) (the specific inhibitor for AC, an enzyme responsible for catalyzing the conversion of cAMP from ATP) or with the PKA inhibitor KT5720 12 h prior to the addition of icariin, and then various osteogenic differentiation markers were analyzed. As shown in Fig. 4*A*, icariin-prompted phosphorylation of PKA and CREB was significantly decreased by DDA, whereas the expression levels of total PKA and CREB were not changed,

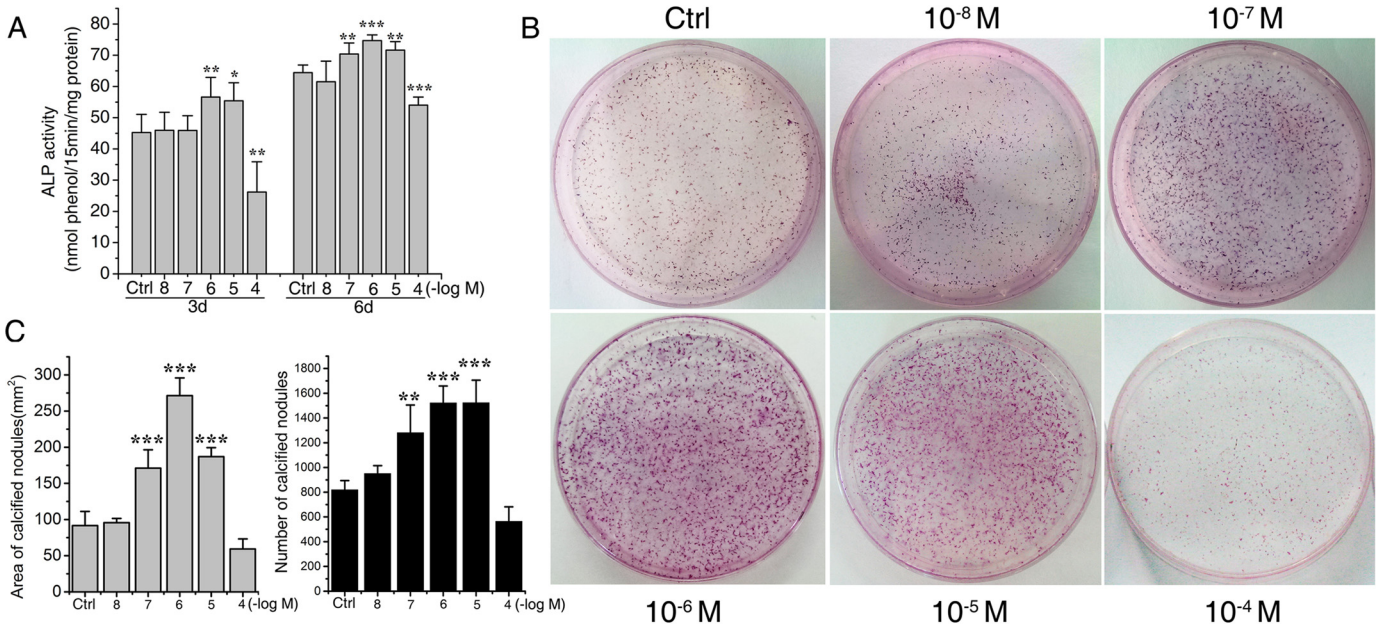

Figure 2. Icariin increased the ALP activities and calcified nodule formation in a dose-dependent manner. *A,* ALP activities of rat calvarial osteoblasts after 3 and 6 days of icariin treatment. *B,* images of calcified nodules stained by alizarin red after 12 days of osteogenic induction culture with icariin. *C,* the areas and numbers of calcified nodules were quantified by Image-Pro Plus 6.0. Each experiment was conducted at least three times independently. Data are represented as mean ± S.D. ($n = 3$); *, $p < 0.05$; **, $p < 0.01$; ***, $p < 0.001$ when compared with control (*Ctrl*).

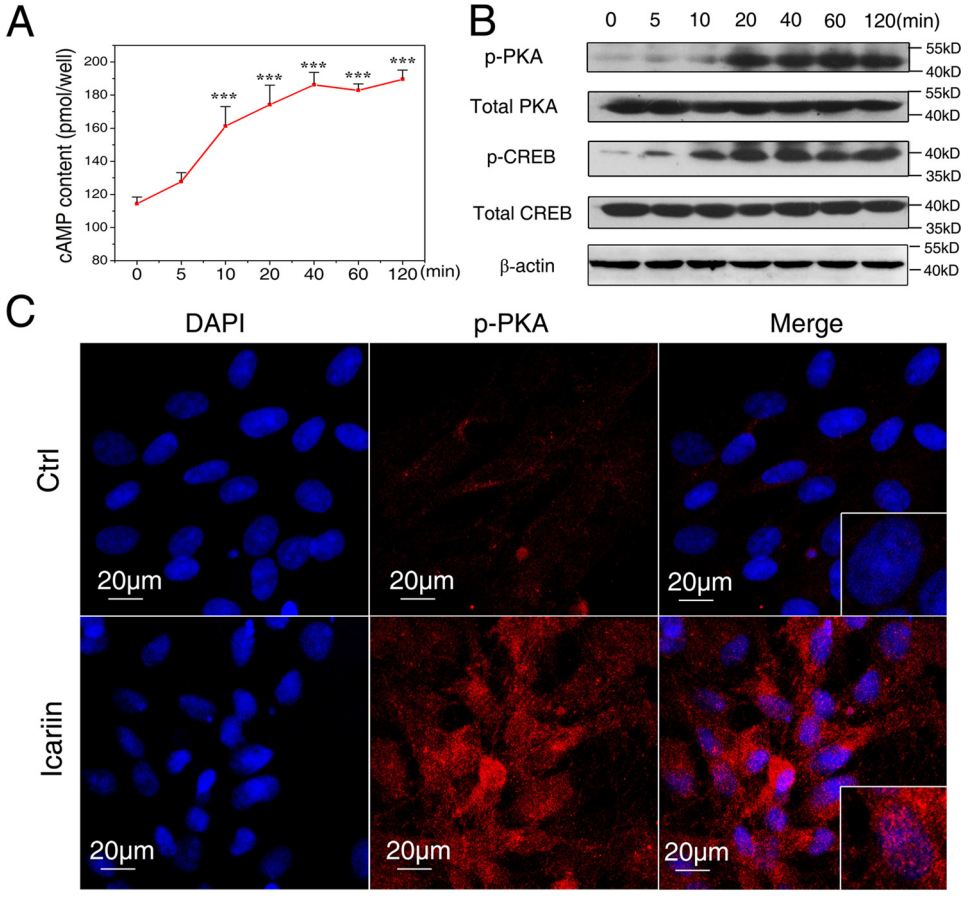

Figure 3. Icariin treatment activated cAMP/PKA/CREB signaling. *A,* the intracellular cAMP contents after exposure to icariin for different time periods. *B,* protein abundance of phosphorylated PKA (*p-PKA*), phosphorylated CREB (*p-CREB*), total PKA and CREB was detected by immunoblotting after different time periods. *C,* the nuclear translocation of *p*-PKA after 120 min of icariin treatment. *p*-PKA is stained *red*, and nuclei are stained *blue* (with DAPI). *Bar* = 20 μm. Each experiment was conducted at least three times independently. Data are represented as mean ± S.D. ($n = 3$); ***, $p < 0.001$ when compared with 0 min.

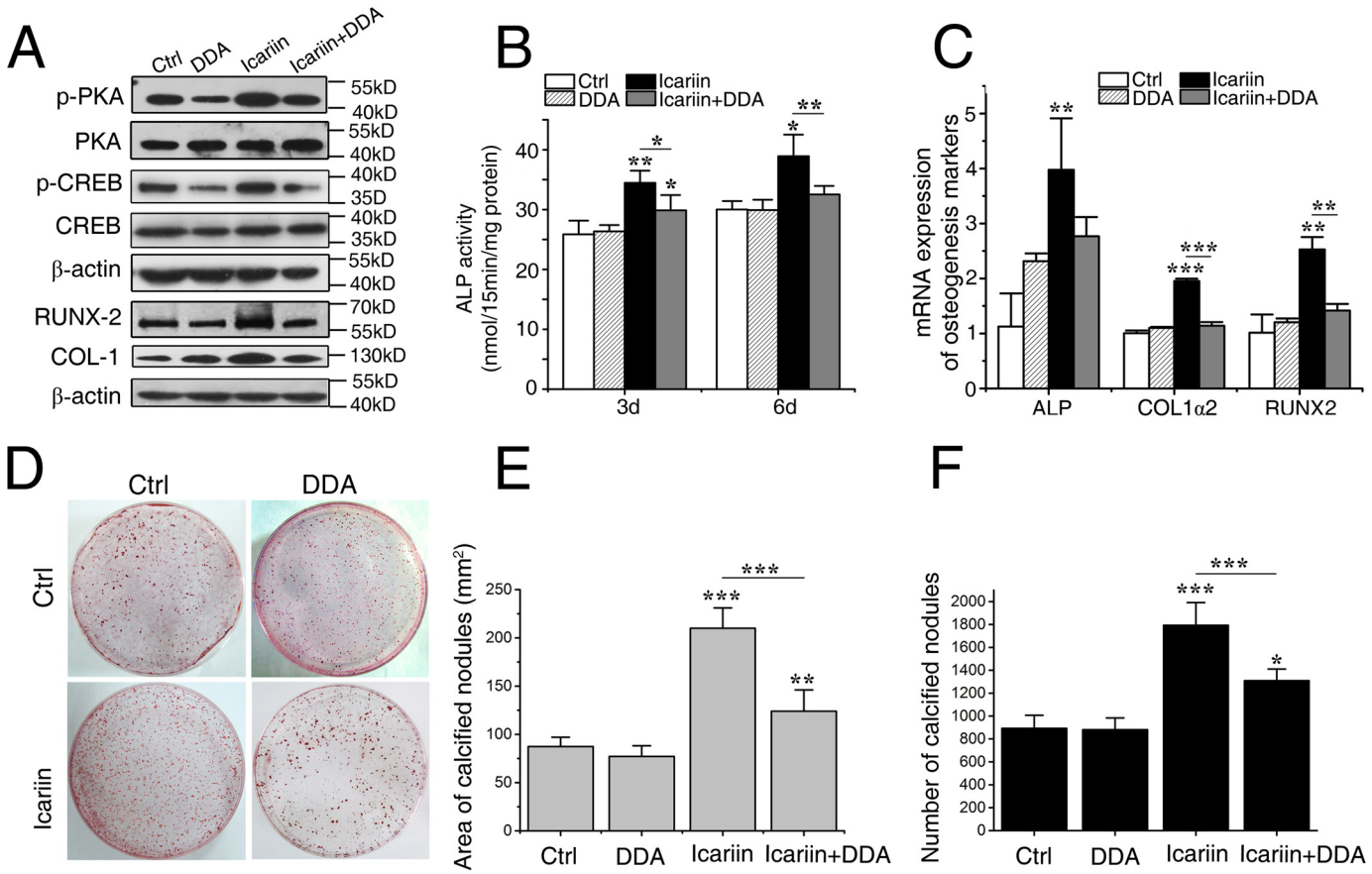

Figure 4. Icariin-induced osteogenesis was inhibited after cAMP/PKA/CREB signaling was blocked. *A,* the protein expression levels of phosphorylated PKA (*p-PKA*), phosphorylated CREB (*p-CREB*), COL-1, and RUNX2 in the cells pretreated by 2′,3′-dideoxyadenosine (*DDA*) (an adenylyl cyclase inhibitor) and treated with/without icariin. *B,* ALP activities after 3 and 6 days. *C,* the relative mRNA expression levels of *ALP*, *COL1α2*, and *RUNX2*. *D,* representative images of calcified nodules formed after 12 days. *E* and *F,* the numbers and areas of calcified nodules. Each experiment was conducted at least three times independently. Data are represented as mean ± S.D. ($n = 3$); *, $p < 0.05$; **, $p < 0.01$; ***, $p < 0.001$, when compared with control (*Ctrl*) or icariin group.

indicating that DDA efficiently blocked icariin-induced activation of the cAMP/PKA/CREB pathway.

The ALP activity was an early marker for osteogenic differentiation. As shown in Fig. 4*B*, ALP activity of the icariin group was significantly higher than that of the control after 3 ($p < 0.01$) and 6 days ($p < 0.05$), and the control group was not significantly different with the DDA alone groups. However, the ALP activity in the icariin + DDA group was dramatically lower than that of the icariin group ($p < 0.01$), demonstrating that the stimulatory effect of icariin on ALP activity was abolished by the AC inhibitor DDA.

Consistently, the mRNA expression levels of *ALP* ($p < 0.01$), collagen 1α2 (*COL1α2*) ($p < 0.001$), and runt-related transcription factor 2 (*RUNX2*) ($p < 0.01$) after 24 h (Fig. 4*C*) and the protein expression levels of COL-1 and RUNX2 after 36 h (Fig. 4*A*) were significantly higher in the icariin group than in the control and DDA group. However, these increases were abolished in the icariin + DDA group. The calcified nodules formed after 12 days showed a similar tendency with the above osteogenic differentiation markers (Fig. 4, *D–F*). The icariin group had the highest number and the largest area of calcified nodules ($p < 0.001$), confirming the stimulatory effect of icariin in the osteogenic differentiation/maturation. However, the effect disappeared in the icariin + DDA group.

When the osteoblasts were pretreated by the PKA inhibitor KT5720, the ALP activity, levels of mRNA expression of *ALP*, *COL1α2*, and *RUNX2*, the protein expression of COL-1 and RUNX2, the number and area of CFU-F_{ALP} colonies, and calcified nodules (supplemental Fig. S4) were all changed in similar tendencies with those of cells pretreated by DDA. These results indicate that the cAMP/PKA/CREB signal pathway was indispensable for the stimulating effect of icariin on osteogenic differentiation and maturation of osteoblasts.

Icariin treatment increased the expression levels of AC2, AC9, and sAC

AC is a GTP-dependent enzyme responsible for catalyzing the conversion of cAMP from ATP, and nine membrane-bound isoforms and a soluble AC (sAC) have been identified. To find the AC isoform(s) responsible for icariin-activated cAMP/PKA/CREB signaling, we first examined the AC isoforms that are expressed in rat calvarial osteoblasts and identified the isoform(s) whose expression was changed after icariin treatment. As shown in Fig. 5*A*, agarose gel electrophoresis of real time RT-PCR products displayed the bands corresponding to *AC1-AC6*, *AC8*, *AC9*, and *sAC*, respectively; however, no band corresponding to *AC7* was found. Quantitative RT-PCR indicated that icariin treatment significantly increased the mRNA

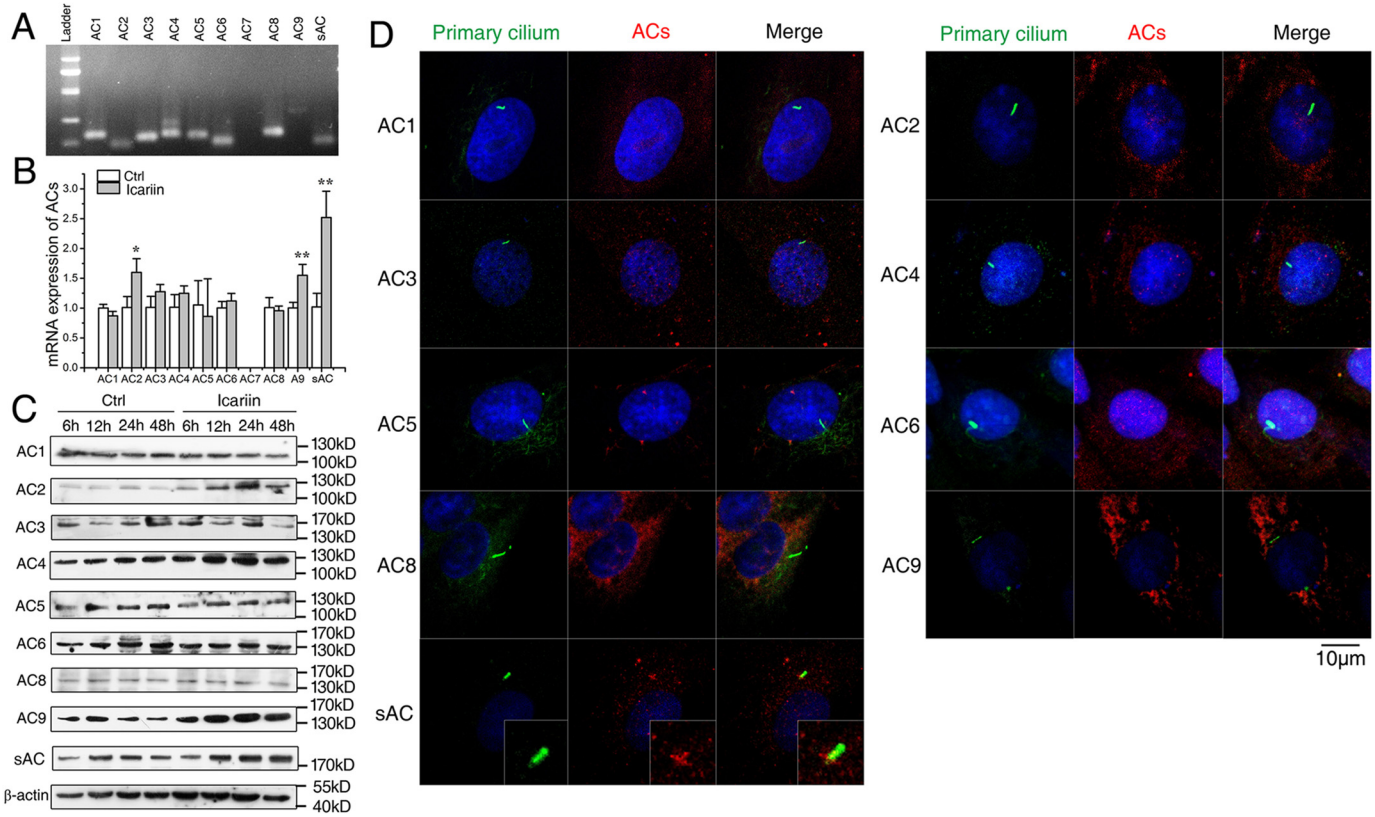

Figure 5. mRNA expression of nine AC isoforms and their immunostaining localization in primary cilia of rat calvarial osteoblasts. *A,* images of agarose gel electrophoresis of real time RT-PCR products of AC1–AC9 and sAC. *B,* mRNA expression of *AC1–AC9* and *sAC* in cells after icariin treatment for 24 h. *C,* protein levels of AC1–AC6, AC8, AC9, and sAC in cells after icariin treatment for 6, 12, 24, and 48 h. *D,* immunostaining localization of nine AC isoforms in primary cilia. Primary cilia are stained *green* (with acetylated α-tubulin), ACs stained *red*, and nuclei stained *blue* (with DAPI). Each experiment was conducted at least three times independently. *Scale bar* = 10 μm. Data are represented as mean ± S.D. ($n = 3$); *, $p < 0.05$; **, $p < 0.01$ when compared with control (*Ctrl*).

expression levels of *AC2* ($p < 0.05$), *AC9* ($p < 0.01$), and *sAC* ($p < 0.01$), and *AC7* was still not detected (Fig. 5*B*). Western blotting analyses of AC1-AC6, AC8, AC9, and sAC showed similar tendencies as those for mRNA expression, and the protein expression levels of AC2, AC9, and sAC were significantly higher in the icariin group than in the control after 12, 24, and 48 h (Fig. 5*C*). These results suggested that AC2, AC9, and sAC may be responsible for the icariin-induced activation of cAMP/PKA/CREB signaling.

Moreover, we examined the effect of icariin on the activity of phosphodiesterase 4 (PDE4), which hydrolyzes cAMP and regulates cAMP concentration. The results showed PDE4 activity was markedly decreased after 15 min of icariin treatment (supplemental Fig. S3*B*), indicating that the increased cAMP level may partly result from the inhibition of PDE4 activity by icariin.

Phosphorylated PKA (p-PKA) and sAC were localized to the primary cilia

Because primary cilia play a role in dynamic flow-induced cAMP pathway in osteocytes (22), we wondered if there is any connection between primary cilia and cAMP/PKA/CREB signaling in icariin-induced osteogenic differentiation of osteoblasts. We first sought to determine which signaling molecules were localized to primary cilia. The distributions of AC1-AC6, AC8, AC9, and sAC, PKA, and *p*-PKA were investigated by immunofluorescence staining in primary cilia of the osteoblasts. Surprisingly, as shown in Fig. 5*D*, we did not find any of the AC isoforms being localized to primary cilia except for sAC, which was always localized at the base of primary cilia. We also found that *p*-PKA was localized in primary cilia, which was preferentially localized to the entire cilia, but sometimes to the ciliary base and/or tip in unstimulated cells (Fig. 6). These results indicate that the activation of cAMP/PKA/CREB signaling may occur at the primary cilia of osteoblasts.

Icariin-activated cAMP/PKA/CREB signaling pathway required the existence of primary cilia

To examine whether primary cilium is needed in icariin-activated cAMP/PKA/CREB signaling, we blocked ciliogenesis using small interfering RNA sequence (siRNA) targeting intraflagellar transport 88 homolog (IFT88), an essential component for the assembly and maintenance of primary cilia. As a result, the mRNA and the protein expression levels of IFT88 were significantly decreased after 24 h compared with the scramble siRNA control (NC) ($p < 0.001$, Fig. 7*A*). Meanwhile, primary cilia became dotted and the number of osteoblasts with primary cilia was significantly reduced ($p < 0.001$, Fig. 7*B*).

Then we quantified the intracellular levels of cAMP, the protein expression levels of AC2, AC9, and sAC, and the phosphorylation levels of PKA and CREB after icariin stimulation. As shown in Fig. 7*D*, the cAMP content of the NC + icariin group was significantly higher than that of the NC group ($p < 0.01$), but had no significant differences with that of the siRNA + icariin group, indicating that primary cilium abrogation had no

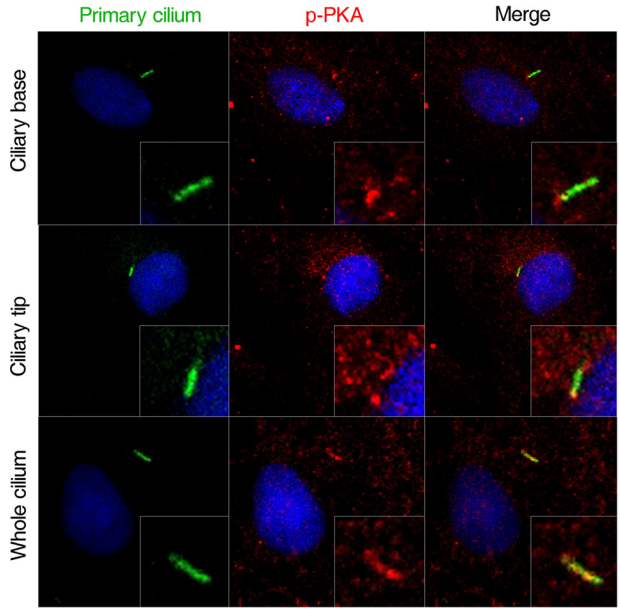

Figure 6. Immunostaining localization of *p*-PKA in primary cilia of rat calvarial osteoblasts. Primary cilium are stained *green* (with acetylated α-tubulin), *p*-PKA stained *red*, and nuclei stained *blue* (with DAPI). *Scale bar* = 10 μm. Each experiment was conducted at least three times independently.

effects on icariin-induced increase in cAMP levels. We also found that there were no significant differences for the expression levels of AC2, AC9, and sAC between NC + icariin group and siRNA + icariin group (Fig. 7*E*). However, the phosphorylation levels of PKA and CREB in the siRNA + icariin group were significantly lower than those of the NC + icariin group, indicating that icariin-promoted phosphorylation of PKA and CREB was blocked in the cells with abrogated primary cilia (Fig. 7*E*). Meanwhile, nuclear translocation of *p*-PKA that happened in the NC + icariin group was obviously suppressed in the siRNA + icariin group (Fig. 7*F*). These results suggested that icariin-activated cAMP/PKA/CREB signaling needs the existence of primary cilia.

Icariin-induced osteogenesis needed the existence of primary cilia

To investigate whether primary cilia play a role in icariin-induced osteogenic differentiation, we blocked ciliogenesis using the same interfering RNA sequence, and then examined the changes in ALP activity and mRNA and protein expression levels related to osteogenesis. As shown in Fig. 7*G*, the promoting effect of icariin on ALP activities disappeared in the cells treated with IFT88 siRNA. The levels of mRNA expression of *ALP*, *COL1α2*, and *RUNX2* and protein expression of COL-1 and RUNX2 displayed the same tendency with that of ALP activity (Fig. 7, *H* and *I*). To avoid the off-target effects of IFT88 siRNA and to verify that the effect of the siRNA on osteogenic differentiation was due to the abrogation of primary cilia, we also inhibited ciliogenesis using 4 mM aqueous chloral hydrate and then examined activation of the cAMP/PKA/CREB pathway and osteogenic differentiation of osteoblasts. It was found that the primary cilia were removed by the pretreatment with aqueous chloral hydrate, and icariin-promoted phosphorylation of PKA and CREB as well as osteogenic differentiation were significantly blocked (supplemental Fig. S5). However, overexpression or knockdown of IFT88 itself had no significant effects on the osteoblastic differentiation (supplemental Fig. S6). These results suggest that icariin-induced osteoblastic differentiation needs the existence of primary cilia.

Icariin administration activated cAMP/PKA/CREB signaling pathway of rats in vivo

To obtain more evidence that icariin promotes bone formation by activating cAMP/PKA/CREB signaling, we examined the expression levels of the signal proteins in tibias of the rats after 2 months of icariin administration. As shown in Fig. 8, the expression levels of *p*-PKA and *p*-CREB in the icariin group were obviously higher than those of the control group, whereas the total PKA and CREB were the same between the two groups. Although the expression levels of AC2 and AC9 were not significantly different between the two groups, the sAC expression level in the icariin group was much higher than that of the control. These results provide further support that icariin promotes bone formation by activating the cAMP/PKA/CREB pathway, and that sAC plays an important role in this process.

Discussion

Icariin is a promising candidate as a natural, alternative way of preventing bone loss due to its potency and low toxicity/side effect profiles in comparison to the potential and in some cases serious adverse effects of existing drugs for treating osteoporosis (2, 7, 28). Here, we found that icariin augmented the attainment of peak bone mass, and therefore might be one of the effective interventions to reduce the risk of developing osteoporosis later in life. However, despite its strong osteogenic activity and safety profiles, the potential of icariin as a clinical drug has been questioned because of its unclear action mechanism. In the current study, icariin was found to exert osteogenic effect by activating the cAMP/PKA/CREB pathway and needs the existence of functional primary cilia on osteoblasts. More remarkably, it was found that icariin-induced activation of cAMP/PKA/CREB signaling was mediated by primary cilia through sAC located at the base of cilia and *p*-PKA located on the whole cilium body.

Many studies have attempted to explain the signaling pathway(s) underlying the osteogenic effect of icariin, for example, the BMP-2/Smad4 signaling, Wnt/β-catenin pathway, and PI3K/AKT/eNOS dependent manner (29–31). As a derivative of flavonoids, icariin was usually thought to be a phytoestrogen and estrogen receptor was its direct molecular target (32). However, because icariin had no binding affinity for the ER receptor (11), we and others tend to think that the estrogen-dependent mechanism may play a secondary role in the osteotropic function of icariin (12–15). There are complex cross-talks among different signaling pathways and many of them play significant roles in icariin-induced osteogenesis. However, the early events, especially the initial signaling events induced by icariin remain unclear. A number of studies indicated that the cAMP pathway is an upstream signaling event. Garcia-Morales *et al.* (33) found that the cAMP effector PKA was responsible for activation of the PI3K/AKT pathway and NO synthase. Suzuki *et al.* (34) reported that cAMP/PKA signaling could

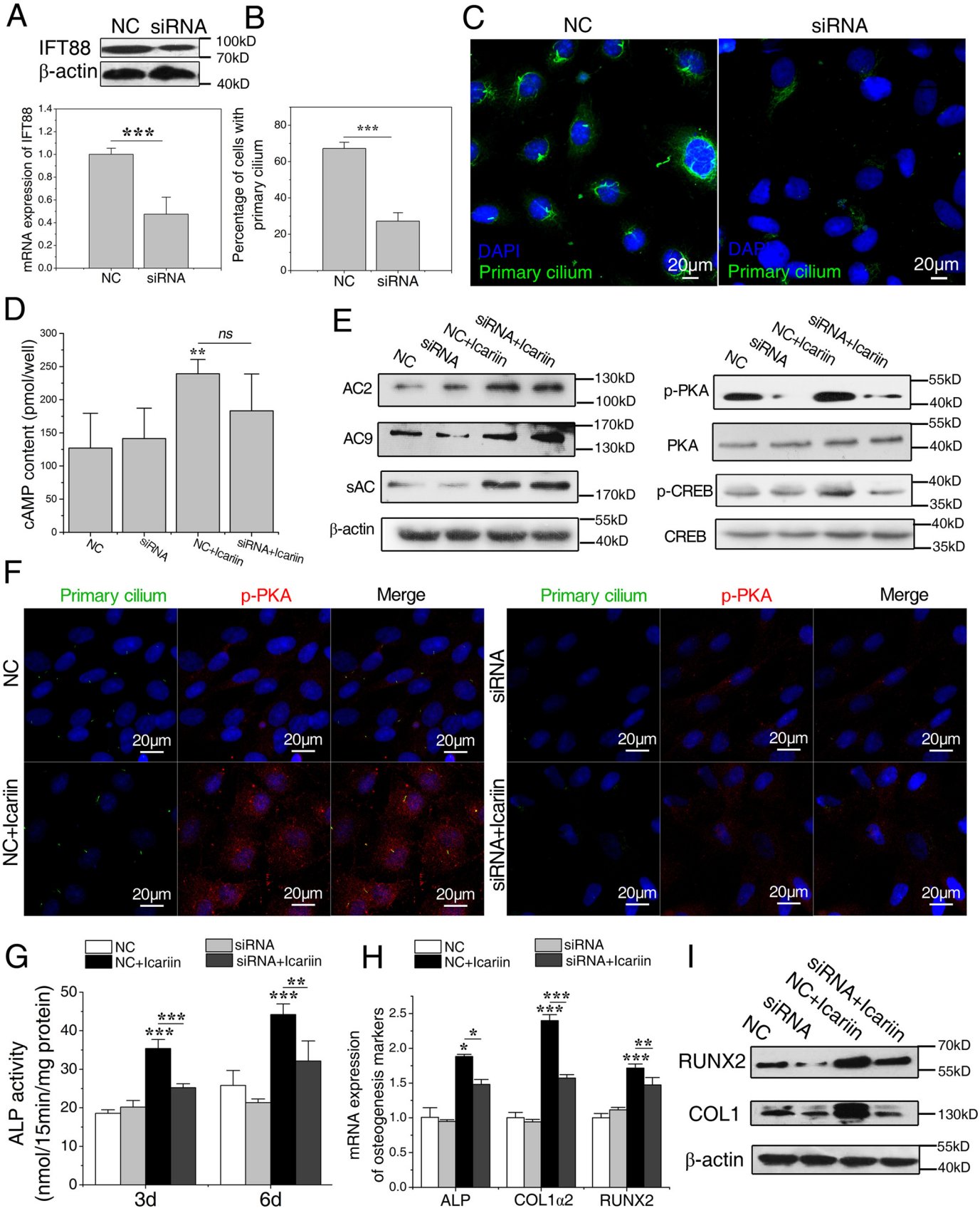
A
NC siRNA
IFT88
β-actin
100kD
70kD
40kD
mRNA expression of IFT88
***
NC
siRNA
B
Percentage of cells with primary cilium
***
NC
siRNA
C
NC
siRNA
DAPI
Primary cilium
20μm
D
cAMP content (pmol/well)
ns
**
NC
siRNA
NC+Icariin
siRNA+Icariin
E
NC
siRNA
NC+Icariin
siRNA+Icariin
AC2
AC9
sAC
β-actin
130kD
100kD
170kD
130kD
55kD
40kD
p-PKA
PKA
p-CREB
CREB
F
Primary cilium
p-PKA
Merge
NC
NC+Icariin
siRNA
siRNA+Icariin
20μm
G
NC
NC+Icariin
siRNA
siRNA+Icariin
ALP activity (nmol/15min/mg protein)
3d
6d
H
mRNA expression of osteogenesis markers
ALP
COL1α2
RUNX2
I
RUNX2
COL1
β-actin
70kD
55kD
130kD

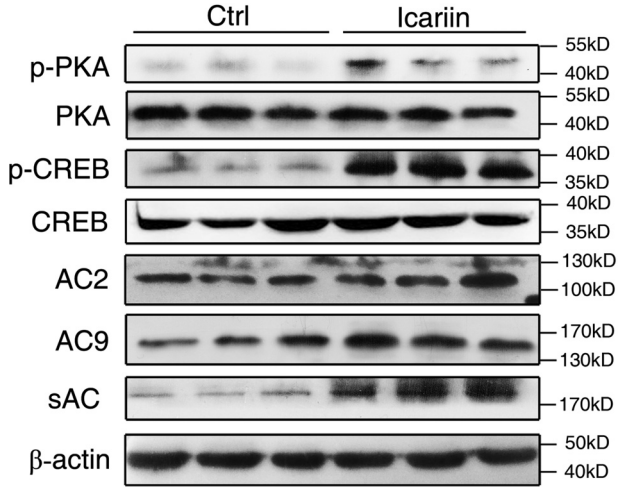

Figure 8. The sAC/cAMP/PKA/CREB signaling pathway was activated in the femurs of rats administrated with icariin or control for 2 months. Shown is the protein abundance of *p*-PKA, *p*-CREB, total PKA, and CREB, AC2, AC9, and sAC as detected by immunoblotting in the femurs. Each experiment was conducted at least three times independently. Data are represented as mean ± S.D. ($n = 6$).

facilitate canonical Wnt signaling. More importantly, intermittent PTH administration regulates cAMP/PKA signaling to enhance the proliferation, osteogenic differentiation, and mineralization of BMSCs and osteoblasts. PTH binding to PTH receptor 1 (PTHR1) stimulates the activation of AC mediated by the G protein subunit $G\alpha_s$, thereby stimulating cAMP production and the subsequent activation of PKA (16–18). Therefore, based on our findings and on these previous studies, we hypothesized that activation of the cAMP-PKA pathway was an initial signaling event in icariin-promoted bone formation.

As a result, we found that icariin treatment activated the cAMP/PKA/CREB signaling pathway, and blocking the pathway by inhibitors of ACs and PKA inhibited icariin-induced osteogenic differentiation and mineralization of osteoblasts. Accompanying activation of the cAMP/PKA/CREB pathway, the levels of mRNA and protein expression of AC2, AC9, and sAC were dramatically increased, whereas no significant changes were found for the expression of other AC isoforms. Western blotting analyses on the protein expression of femurs isolated from the rats administered with icariin for 2 months revealed that among three AC isoforms (AC2, AC9, and sAC), only sAC was increased significantly. Meanwhile, the phosphorylation levels of PKA and CREB were greatly promoted, indicating activation of the sAC/cAMP/PKA/CREB signaling pathway *in vivo*. More importantly, we found that sAC and *p*-PKA were localized at primary cilia, and when primary cilia of osteoblasts were abrogated, cAMP/PKA/CREB signaling would no longer be activated and the osteogenic differentiation induced by icariin would be inhibited. These results demonstrated that icariin stimulates osteogenic differentiation by activating the cAMP signaling pathway that was localized at primary cilia.

Primary cilia, extending from the cell surface like an antenna, act as a sensor to receive the mechanical and chemical stimuli from the extracellular environment (20). As a tiny organelle of 200–300 nm in diameter and a few micrometers long, the primary cilium has a much higher surface–volume ratio than the cell body, and therefore accommodates more receptors, ion channels, and signal molecules in the membrane or cavity, which make the signaling cross-talk more effective or efficiently activated by extracellular stimuli (19–21). The primary cilium is essential for chemical stimulus-induced bone formation. Labor *et al.* (35) found that the recruitment of mesenchymal stem cells in bone relies on proper formation of the cilium, and the canonical TGF-β signaling was associated with activation of SMAD3 at the ciliary base. Bodle *et al.* (36) reported that the primary cilium acted as a chemical antenna to regulate osteogenesis from human adipose–derived stem cells. We recently reported that the primary cilium is required for the stimulating effect of icaritin, a metabolite of icariin, on osteogenic differentiation and mineralization of osteoblasts (37).

In the present study, the primary cilium was found associated with the cAMP/PKA/CREB signaling pathway through *p*-PKA localized at the whole ciliary body and sAC localized at the ciliary base. Previous studies have shown that PKA activation could mediate the length of primary cilia and play a significant role in ciliogenesis (38). Besschetnova *et al.* (38) reported that a decreased intracellular Ca^{2+} or an increased cyclic AMP content would activate PKA, and then increase the anterograde IFT88 particle transport velocities to elongate the primary cilium. We found that *p*-PKA was localized to the entire cilia and sometimes to the ciliary base and/or tip in cultured osteoblasts. Furthermore, abrogating of primary cilia using IFT88 knockout significantly inhibited icariin-induced phosphorylation of PKA and activation of CREB. These findings indicate that PKA plays a key role in primary cilium–dependent bone formation induced by icariin.

There have been several adenylyl cyclases reported to be localized to the primary cilium. For example, AC3 localizes to primary cilia of mouse brain cells and AC5/6 to primary cilia of the renal epithelial cells, and the functional cAMP-signaling pathway is involved in controlling the ciliary channel function and the sensory function of the primary cilium (22, 39). In particular, Kwon *et al.* (22) found that AC6, instead of other isoforms, localizes to the primary cilium and mediates flow-induced decreases in cAMP in osteocytes. Besides, AC6 was found to mediate loading-induced bone adaptation *in vivo* (22).

Figure 7. Icariin-induced activation of cAMP/PKA/CREB signaling and osteogenesis in rat calvarial osteoblasts require the existence of primary cilia. *A,* the mRNA and the protein expression levels of IFT88 in cells transfected by negative control siRNA (*NC group*) or IFT88 siRNA (*siRNA group*). *B,* the percentage of cells with primary cilia after the transfection. *C,* primary cilia of the transfected osteoblasts. The primary cilium was stained with acetylated α-tubulin (*green*), and DNA stained with DAPI (*blue*). *Bar* = 20 μm. *D,* the intracellular cAMP contents in the transfected osteoblasts after icariin treatment for 120 min. *E,* protein abundance of AC2, AC9, and sAC, *p*-PKA, *p*-CREB, total PKA, and CREB in the transfected osteoblasts after icariin treatment. *F,* the nuclear translocation of *p*-PKA in the transfected osteoblasts after exposure to icariin. *G,* ALP activity in the transfected osteoblasts after 3 and 6 days of icariin supplement. *H* and *I*, the relative mRNA expression levels of *ALP*, *COL1α2*, and *RUNX2* (*H*) and protein expression levels of COL1 and RUNX2 (*I*) in transfected osteoblasts after 3 and 6 days of icariin supplement. Each experiment was conducted at least three times independently. Data are represented as mean ± S.D. ($n = 3$); *, $p < 0.05$; **, $p < 0.01$; ***, $p < 0.001$ when compared with NC or NC + icariin group.

However, we did not find AC6 and any of other isoforms in the primary cilia of rat calvarial osteoblasts except for sAC.

The sAC was recently identified as a widely expressed intracellular source of cAMP in mammalian cells, and is evolutionarily, structurally, and biochemically distinct from the transmembranous adenylyl cyclases (tmAC) (40, 41). Although G-protein–coupled receptors and heterotrimeric G proteins regulate tmAC, the regulation of sAC is completely different. sAC is directly activated by HCO_3^- and Ca^{2+}. Ca^{2+} and bicarbonate synergistically activate sAC and lead to significant changes in cellular cAMP levels (42). Furthermore, whereas tmACs are restricted to membranes, sAC can be localized throughout the cell and is found in mitochondria, nuclei, centrioles, and mitotic spindle (41, 43). At these locations, sAC was anchored together with PKA by scaffold proteins, such as protein kinase A anchoring proteins (AKAP), allowing local utilization (44). The current work represents the first time study where both PKA and sAC were found localized in primary cilia of osteoblasts, and therefore PKA and sAC may be anchored together to play a role in icariin-induced bone formation process.

sAC has been reported to be involved in bone metabolism. Geng *et al.* (45) found that the differentiation of multinucleated osteoclasts was decreased by HCO_3^- in a dose-dependent manner, and it was blocked by either an inhibitor of sAC or sAC knockdown via a specific siRNA. The HCO_3^- effect on bone volume fraction of cultured mouse calvaria was blocked by the sAC inhibitor. Reed *et al.* (46) reported sAC was associated with low spinal BMD in hypercalciuric patients, and Ichikawa *et al.* (47) found a modest association between sAC polymorphism and spinal areal BMD in premenopausal white women. Our findings are consistent with the above results, indicating that sAC expression is essential for bone formation and should be the early signaling event mediator in icariin-promoted bone formation.

However, we do not know why the sAC expression level was not affected by the abrogation of primary cilia, although the level of PKA phosphorylation was markedly decreased. It must also be emphasized that although the signaling protein expression levels of the cAMP/PKA/CREB pathway were found to be significantly increased in femurs of the rats administered icariin, we could not rule out the possibility that the increase was due to the number of osteoblasts because the results could not be corrected by the number of total osteoblasts. Finally, we still do not know the direct molecular binding target for icariin. One potential method we could use to fish out the binding target is by employing biotin-labeled icariin, out of which the icariin-receptor compound and the interacting proteins would be collected by streptavidin Dynabeads, and the receptor may be recognized by mass spectrometry and related analysis.

In summary, the current study has elucidated a novel molecular mechanism of icariin osteogenic action in which it stimulates the bone formation through activating the cAMP/PKA/CREB signaling pathway that is related to primary cilia due to its localization of sAC and PKA. Further studies are required to clarify the exact roles of sAC and other signal molecules in the whole signaling process in primary cilia induced by icariin or other bone formation promoters.

Experimental procedures

Animal experiments

Twenty 1-month old female S.D. rats were obtained from the Animal Breeding Center, Gansu University of Traditional Chinese Medicine (Lanzhou, China). Animal experiments were approved by Animal Ethics Committee of Lanzhou General Hospital and were conducted according to the NIH Guidelines for the Care and Use of Laboratory Animals. Rats were housed 5 rats per cages (465 × 300 × 150 mm) with 12-h light/dark illumination cycles at a constant temperature of 25 ± 2 °C and humidity 50–70%. The rats were randomly divided into two groups, the icariin group (n = 8), which was orally gavaged with 25 mg/kg of icariin (National Institute for the Control of Pharmaceuticals and Biological Products, Beijing, China, purity>99%) every day except for Sunday, and the control group (n = 8), which was gavaged with an equal volume of ddH_2O. After 2 months, the rats were anesthetized by intraperitoneal injection of 10% chloral hydrate (0.3 ml/kg), and the blood samples were collected from the aorta and centrifuged to obtain the serum. The dissected femurs and tibia were cleaned of adhering soft tissues and used to perform biomechanical tests, micro-CT scan, and bone histomorphometric analyses. The organs including liver, kidney, spleen, and uterus were weighted, fixed in 10% formalin, and used for pathological examination.

Measurement of BMD

The BMD of left femurs and vertebra were measured by a DEXA (Prodigy, GE Healthcare, Madison, WI) equipped with enCORE software (GE Healthcare) for bone assessment in small animals. The scan resolution was 1.0 × 1.0 mm and scan speed was 10 mm/s. The measurements with repositioning of the bones were repeated three times to calculate the means.

Bone biomechanics test

The biomechanical properties of femurs and vertebrae were analyzed by a three-point bending test and compression test, respectively, in a material testing machine (AG-IS, Shimadzu, Kyoto, Japan). The bone samples were cleaned of soft tissue and kept wet by phosphate-buffered saline (PBS)-soaked gauze before the testing. The femur was mounted on two inferior supports and a load was applied to the mid-shaft on its anterior surface until fractured. L5 vertebrae were trimmed of bony processes and the vertebral body was placed between the compaction discs. The compression was given along the cephalocaudal axis. The parameters of ultimate load (N) were collected by a computer connected to the machine.

Biochemical analyses

The bone formation marker osteocalcin in serum was measured with Rat-MID™ Osteocalcin EIA kit, and the bone resorption maker TRACP 5b was analyzed by a RatTRAP™ (TRAcP 5b) ELISA kit. Both kits are the products of IDS (Immunodiagnostic Systems, Tyne & Wear, UK).

Micro-computed tomography assessment

The freshly isolated right femurs were assessed using micro-CT (Skyscan 1176, Bruker, Aarsellar, Belgium) at 18-μm

resolution with 70 kV, 114 uA. The trabecular bone region of distal femora was chosen for analysis of the micro-architectural parameters, including Tb.Th, Tb.N, and Tb.Sp, BV/TV, and BMD. NR Econ software version 1.6 was used for the 3D reconstruction and viewing of images.

Bone histomorphometric analysis

The tibias were cleaned of adhering soft tissues and fixed in 4% paraformaldehyde for 24 h. They were then dehydrated through a graded ethanol series and embedded un-decalcified in methyl methacrylate. The embedded un-decalcified tibias were cut at 10-μm thicknesses using a microtome (Leica SP 1600, Germany). The trabecular bone region of proximal tibia was stained with picronitric acid and pinkish red for histomorphometric analyses. Images of the distracted zones were captured under $\times$4 magnifications using a light microscope (BX51, Olympus Co., Tokyo, Japan).

Osteoblast isolation and culture

The rat calvarial osteoblasts were isolated from neonatal S.D. rats (within 48 h after birth, Animal Breeding Center, Gansu University of Traditional Chinese Medicine, Lanzhou, China) as previously described (48). Briefly, the calvarias were dissected aseptically and minced to about 1-mm^3 pieces, digested at 37 °C with 0.25% trypsin twice, 15 min for each time, and then with 1 mg/ml of collagenase II (Sigma) for six times, 20 min for each time. The released cells from the last three digests were filtered through a 200-μm sieve to remove bone debris and collected by centrifugation at 1000 rpm for 5 min. The collected cells were cultured in DMEM (Gibco) supplemented with 10% FBS (Gibco). The cultures were maintained in a 5% humidified CO_2 atmosphere and medium was changed every 2–3 days. When the cells reached 70–80% confluence, they were subcultured at 2×10^4 cells/ml in 60-mm dishes and used for various assays as described below. For immunostaining experiments, cells were grown on 76 $\times$ 48 $\times$ 1-mm UV-transparent quartz slides (Fisher Scientific, Waltham, MA).

Cell treatments

To determine the optimal concentration of icariin in enhancing osteogenesis, the osteoblasts were cultured in the osteogenic medium (containing 10^{-8} M dexamethasone, 10 mM β-glycerophosphate, and 0.1 mM ascorbic acid-2-phosphate), and icariin was supplemented at concentrations of 10^{-8}, 10^{-7}, 10^{-6}, 10^{-5}, and 10^{-4} M, respectively. ALP activity and number and areas of calcified nodules of the cultures after different days were determined.

To analyze functions of the cAMP/PKA/CREB signaling in mediating icariin-induced osteogenic differentiation of osteoblasts, the cells were pretreated with 10^{-5} M of the AC inhibitor DDA or PKA inhibitor KT5720 (Sigma) (49, 50). Briefly, after subculturing for 12 h in the osteogenic medium, the osteoblasts were treated with or without 10^{-6} M icariin and inhibitors (solubilized in DMSO, with the final concentration of DMSO being less than 0.05%). Treatment effects on osteogenic differentiation were examined at different time points by analyzing markers including ALP activity, *COL1α2*, and *RUNX2* mRNA and protein expression levels as well as the formation of calcified nodules. To remove primary cilia by an alternative method, 4 mM aqueous chloral hydrate (Sigma) was added to the culture media of osteoblasts for 48 h, the cells were washed three times with PBS, and fresh medium was added for 24 h before icariin treatment (25).

ALP activity measurement and calcified nodule assay

After 3 and 6 days of icariin treatment, the cultures were rinsed twice with sterile PBS and the ALP activities were measured biochemically with a modified method of King using a commercial kit (Nanjing Jiancheng Bioengineering Ltd., Nanjing, China), with the results expressed as nanomole of phenol/15 min/mg of protein. The calcified nodules formed by osteoblasts were assessed after 12 days with or without icariin. Briefly, the cells were fixed for 10 min by 4% paraformaldehyde and stained by 0.1% alizarin red for 1 h at 37 °C, the numbers and total areas of red-calcified nodules were measured by Image-Pro Plus 6.0 software.

cAMP quantification

For measuring cAMP contents, cells seeded in 60-mm culture dishes were incubated for 20 min with 200 μl of ice-cold 0.1 M HCl with 0.5% Triton X-100 to inhibit phosphodiesterase activity. Then the cells were scraped off and dissociated to a homogenous suspension by pipetting, from which a supernatant was obtained after centrifugation at 12,000 rpm for 10 min, and was used for measurement of cAMP content using a cAMP enzyme immunoassay kit (Enzo Life Sciences, Farmingdale, NY). All samples and standards were run in triplicate and repeated 3 times.

Immunofluorescent staining and confocal imaging

Cells were fixed in 4% paraformaldehyde and permeabilized with 0.2% Triton X-100 (PBST) for 10 min and blocked with 5% bovine serum albumin in PBST for 30 min. Immunostaining was carried out using primary antibodies targeted against acetylated α-tubulin (1:500, Abcam, Cambridge, UK), phosphorylated PKA catalytic subunits (1:200, Abcam), or AC1-AC6, AC8, AC9, and sAC (AC6: 1:200, Santa Cruz Biotechnology, Dallas, TX; all others: 1:200, Abcam). Secondary antibodies were FITC-labeled goat anti-mouse IgG and rhodamine-labeled goat anti-rabbit IgG (1:500, KPL, Gaithersburg, MD). Cellular nuclear DNA was stained with DAPI (1:100,000, Sigma). Images were acquired using a Zeiss LSM 700 Meta laser scanning confocal microscope with a $\times$40 1.4-NA Plan-Apochromat oil immersion objective. To avoid bleed-through effects in double/triple-staining experiments, each dye was scanned independently in a multitracking mode.

Real-time quantitative PCR analysis

Total cellular RNA was extracted using TRIzol reagent (Takara Biotechnology, Dalian, China). To remove any DNA contamination, RNA samples were treated with DNase I (Takara). Single-stranded cDNA was synthesized from total RNA with the Primescrip^{TM} RT reagent kit (Takara). The mRNA expression levels of the following osteogenesis-related genes and internal control GAPDH were analyzed by real-time PCR performed on an ABI Biosystems 7300 (Applied Biosys-

Table 1
Primer sequences used for real-time RT-PCR analyses

Gene	Forward primer (5′-3′)	Reverse primer (5′-3′)
COL1α2	TGGCAAGGCCGGTGAAGATA	TGACCAGGAAGCCCTCGGACT
RUNX2	GCACCCAGCCCATAATAGA	TTGGAGCAAGGAGAACCC
ALP	CGCTTTGACCAACAGTGTGGA	CCTTGTAACCAGGCCCGTTG
IFT88	TCAGGCTATTGAGTGGCT	TCTCGCAGAACTGGGTAT
AC1	CCAACGTAATGACCTGTGAGGATG	AGGCGGCTGATGTACCTGTTG
AC2	GCCAGCAGAATGGACAGCAC	GCCAAGCGTCTGCAAGATGA
AC3	CCTGGGCCATGTTAGCCATC	TACAGCCACCGTCCAGCTCTATC
AC4	AGCTGGTGCTAATGCTCAATGAA	CAATTGATGGCGTGGTCAGG
AC5	TGCCATGGAGATGAAAGCAGA	TGGGATGCCAGGCTAGTGAAG
AC6	AAGGACTCTAAGGCATTCCGACA	CCACCTCATCCTCAGGGTTCA
AC7	CTGATGAGCAAGCTGGATGGAA	CTGATGAGCAAGCTGGATGGAA
AC8	TGGAATCCATTCAGGCTCTGTG	CCAGTGTGGCTTTGGAAATGTG
AC9	ACCTACCTTTACCCAAAGTGCACGGACAAT	CTCGGCGCTGCCTCACACACTCTTTGAGAC
AC10	GTCACCTCCAGCATCGCTCA	AATGATAGCAGCACACCTCACCAG
GAPDH	TATCGGACGCCTGGTTAC	CTGTGCCGTTGA ACTTGC

tems, Singapore). All reactions were carried out in triplicate and expression data (after being calibrated with GAPDH levels) were analyzed using the $2^{-\triangle\triangle CT}$ method. Optimal oligonucleotide primers used in the above PCR assays were designed and synthesized by Takara Biotechnology based on published rat cDNA sequences (Table 1).

Western blotting

Cells were harvested and homogenized in RIPA lysis buffer (Solarbio, Beijing, China), and supernatant was obtained after centrifugation at 4 °C for 15 min at 12,000 rpm. Total cellular protein was isolated and protein content was quantified by a BCA kit (Solarbio). Samples were separated by SDS-PAGE (Solarbio) and transferred onto PVDF membranes. Membranes were blocked in 5% nonfat milk and probed overnight at 4 °C with rabbit anti-phosphorylated PKA catalytic subunit (1:1,000, Abcam), rabbit anti-PKA (1:1,000, Abcam), mouse anti-CREB (1:1,000, Abcam), mouse anti-phosphorylated CREB (1:1,000, Abcam), rabbit anti-COL1 (1:1,000, Abcam), rabbit anti-RUNX2 (1:1,000, Abcam), rabbit anti-AC1-AC6 and AC8, AC9, and sAC (AC6: 1:500, Santa Cruz, CA; all others: 1:1,000, Abcam), or rabbit anti-IFT88 (1:500, Santa Cruz Biotechnology). Bound primary antibodies were detected by chemiluminescent detection of HRP-conjugated goat anti-rabbit antibodies (1:10,000, Bioworld, Nanjing, China).

For measuring the levels of protein expression in rat femurs, freshly isolated femurs were cleaned of soft tissue, rinsed of bone marrow, and ground into powders in liquid nitrogen. Total protein was extracted using RIPA lysis buffer and the expression of *p*-PKA, PKA, *p*-CREB, CREB, AC2, AC9, and AC10 (Abcam) were examined using Western blotting as above.

RNA interference of IFT88

To prevent cilium formation by knockdown of IFT88 (51, 52), a protein required for formation and assembly of cilia, oligonucleotides of siRNA targeting *IFT88* (siRNA, 5′-GGAUAUGGGUCCAAGACAUCC-3′; siRNA2, 5′-GGACCUAACCUACUCCGUUCU-3′) and a corresponding negative control siRNA (Invitrogen, Shanghai, China) were synthesized and cloned into the pENTR^{TM}/U6 vectors (Invitrogen) and transfected into osteoblasts using Lipofectamine 2000 (Invitrogen). Assays for evaluating gene silencing efficiency were performed 24 h after transfection by RT-PCR and Western blotting. The green fluorescent protein (GFP) was also used as an indicator for success of transfection.

Statistical analyses

Statistical analyses were performed using SPSS 20.0 (SPSS Inc., Chicago, IL). Data were expressed as mean ± S.D. Statistical differences of data were analyzed using Bonferroni modification of Student's *t* test for two groups and one-way analysis of variance followed by a Dunnett's or LSD post hoc test for multiple groups. Differences between means were considered statistically significant when $p < 0.05$, 0.01, or 0.001.

Author contributions—K. C., J. W., and W. S. designed the experiments, analyzed data, and wrote the paper. W. S., Y. W., Y. G., J. Z., and Z. W. performed the experiments. H. M. and X. M. interpreted the data. C. J. X. interpreted the data and reviewed the manuscript.

References

1. Wang, L., Li, Y., Guo, Y., Ma, R., Fu, M., Niu, J., Gao, S., and Zhang, D. (2016) *Herba epimedii*: an ancient Chinese herbal medicine in the prevention and treatment of osteoporosis. *Curr. Pharm. Des.* **22,** 328–349
2. Chen, K. M., Ge, B. F., Ma, H. P., Liu, X. Y., Bai, M. H., and Wang, Y. (2005) Icariin, a flavonoid from the herb *Epimedium* enhances the osteogenic differentiation of rat primary bone marrow stromal cells. *Pharmazie* **60**, 939–942
3. Indran, I. R., Liang, R. L., Min, T. E., and Yong, E. L. (2016) Preclinical studies and clinical evaluation of compounds from the genus *Epimedium*, for osteoporosis and bone health. *Pharmacol. Ther.* **162,** 188–205
4. Chen, K. M., Ge, B. F., Liu, X. Y., Ma, P. H., Lu, M. B., Bai, M. H., and Wang, Y. (2007) Icariin inhibits the osteoclast formation induced by RANKL and macrophage-colony stimulating factor in mouse bone marrow culture. *Pharmazie* **62,** 388–391
5. Nian, H., Ma, M. H., Nian, S. S., and Xu, L. L. (2009) Antiosteoporotic activity of icariin in ovariectomized rats. *Phytomedicine* **16,** 320–326
6. Zheng, D., Peng, S., Yang, S. H., Shao, Z. W., Yang, C., Feng, Y., Wu, W., and Zhan, W. X. (2012) The beneficial effect of Icariin on bone is diminished in osteoprotegerin-deficient mice. *Bone* **51,** 85–92
7. Zhang, G., Qin, L., and Shi, Y. (2007) Epimedium-derived phytoestrogen flavonoids exert beneficial effect on preventing bone loss in late postmenopausal women: a 24-month randomized, double-blind and placebo-controlled trial. *J. Bone Miner. Res.* **22,** 1072–1079
8. Weaver, C. M., Gordon, C. M., Janz, K. F., Kalkwarf, H. J., Lappe, J. M., Lewis, R.,O'Karma, M., Wallace, T. C., and Zemel, B. S. (2016) The National Osteoporosis Foundation's position statement on peak bone mass development and lifestyle factors: a systematic review and implementation recommendations. *Osteoporosis Int.* **27,** 1281–1386

9. Song, L., Zhao, J., Zhang, X., Li, H., and Zhou, Y. (2013) Icariin induces osteoblast proliferation, differentiation and mineralization through estrogen receptor-mediated ERK and JNK signal activation. *Eur. J. Pharmacol.* **714,** 15–22
10. Rickard, D. J., Monroe, D. G., Ruesink, T. J., Khosla, S., Riggs, B. L., and Spelsberg, T. C. (2003) Phytoestrogen genistein acts as an estrogen agonist on human osteoblastic cells through estrogen receptors α and β. *J. Cell. Biochem.* **89,** 633–646
11. Xiao, H. H., Fung, C. Y., Mok, S. K., Wong, K. C., Ho, M. X., Wang, X. L., Yao, X. S., and Wong, M. S. (2014) Flavonoids from *Herba epimedii*, selectively activate estrogen receptor alpha (ERα) and stimulate ER-dependent osteoblastic functions in UMR-106 cells. *J. Steroid Biochem. Mol. Biol.* **143,** 141–151
12. Mok, S. K., Chen, W. F., Lai, W. P., Leung, P. C., Wang, X. L., Yao, X. S., and Wong, M. S. (2010) Icariin protects against bone loss induced by oestrogen deficiency and activates oestrogen receptor-dependent osteoblastic functions in UMR 106 cells. *Br. J. Pharmacol.* **159,** 939–949
13. Shi, W. G., Ma, X. N., Xie, Y. F., Zhou, J., and Chen, K. M. (2014) Icariin promote maturation of osteoblasts *in vitro* by an estrogen-independent mechanism. *China J. Chinese Materia Medica* **39,** 2704–2709
14. Ma, H. P., Ming, L. G., Ge, B. F., Zhai, Y. K., Song, P., Xian, C. J., and Chen, K. M. (2011) Icariin is more potent than genistein in promoting osteoblast differentiation and mineralization *in vitro*. *J. Cell. Biochem.* **112,** 916–923
15. Ming, L. G., Chen, K. M., and Xian, C. J. (2013) Functions and action mechanisms of flavonoids genistein and icariin in regulating bone remodeling. *J. Cell. Physiol.* **228,** 513–521
16. Isogai, Y., Akatsu, T., Ishizuya, T., Yamaguchi, A., Hori, M., Takahashi, N., and Suda, T. (1996) Parathyroid hormone regulates osteoblast differentiation positively or negatively depending on the differentiation stages. *J. Bone Miner. Res.* **11,** 1384–1393
17. Koh, A. J., Beecher, C. A., Rosol, T. J., and McCauley, L. K. (1999) 3′,5′-Cyclic adenosine monophosphate activation in osteoblastic cells: effects on parathyroid hormone-1 receptors and osteoblastic differentiation *in vitro*. *Endocrinology* **140,** 3154–3162
18. Chen, B., Lin, T., Yang, X., Li, Y., Xie, D., and Cui, H. (2016) Intermittent parathyroid hormone (1–34) application regulates cAMP-response element binding protein activity to promote the proliferation and osteogenic differentiation of bone mesenchymal stromal cells, via the cAMP/PKA signaling pathway. *Exp. Ther. Med.* **11,** 2399–2406
19. Singla, V., and Reiter, J. F. (2006) The primary cilium as the cell's antenna: singaling at a sensory organelle. *Science* **313,** 629–633
20. Satir, P., Pedersen, L. B., and Christensen, S. T. (2010) The primary cilium at a glance. *J. Cell Sci.* **123,** 499–503
21. Mukhopadhyay, S., Wen, X., Ratti, N., Loktev, A., Rangell, L., Scales, S. J., and Jackson, P. K. (2013) The ciliary G-protein-coupled receptor Gpr161 negatively regulates the sonic hedgehog pathway via cAMP signaling. *Cell* **152,** 210–223
22. Kwon, R. Y., Temiyasathit, S., Tummala, P., Quah, C. C., and Jacobs, C. R. (2010) Primary cilium-dependent mechanosensing is mediated by adenylyl cyclase 6 and cyclic AMP in bone cells. *FASEB J.* **24,** 2859–2868
23. Xiao, Z., Zhang, S., Mahlios, J., Zhou, G., Magenheimer, B. S., Guo, D., Dallas, S. L., Maser, R., Calvet, J. P., Bonewald, L., and Quarles, L. D. (2006) Cilia-like structures and polycystin-1 in osteoblasts/osteocytes and associated abnormalities in skeletogenesis and Runx2 expression. *J. Biol. Chem.* **281,** 30884–30895
24. Hoey, D. A., Chen, J. C., and Jacobs, C. R. (2012) The primary cilium as a novel extracellular sensor in bone. *Front. Endocrinol.* **3,** 75
25. Malone, A. M., Anderson, C. T., Tummala, P., Kwon, R. Y., Johnston, T. R., Stearns, T., and Jacobs, C. R. (2007) Primary cilia mediate mechanosensing in bone cells by a calcium-independent mechanism. *Proc. Natl. Acad. Sci. U.S.A.* **104,** 13325–13330
26. Yan, J. L., Zhou, J., Ma, H. P., Ma, X. N., Gao, Y. H., Shi, W. G., Fang, Q. Q., Ren, Q., Xian, C. J., and Chen, K. M. (2015) Pulsed electromagnetic fields promote osteoblast mineralization and maturation needing the existence of primary cilia. *Mol. Cell. Endocrinol.* **404,** 132–140
27. Marion, V., Schlicht, D., Mockel, A., Caillard, S., Imhoff, O., Steoetzel, C., Stoetzel, C., van Dijk, P., Brandt, C., Moulin, B., and Dollfus, H. (2011) Bardet-Biedl syndrome highlights the major role of the primary cilium in efficient water reabsorption. *Kidney Int.* **79,** 1013–1025
28. Ma, X. N., Zhou, J., Ge, B. F., Zhen, P., Ma, H. P., Shi, W. G., et al. (2005) Icariin induced osteoblast differentiation and mineralization without dexamethasone *in vitro*. *Planta Medica* **60,** 939–942
29. Wang, J., Tao, Y., Ping, Z., Zhang, W., Hu, X., Wang, Y.,Wang, L., Shi, J., Wu, X., Yang, H., Xu, Y., and Geng, D. (2016) Icariin attenuates titanium-particle inhibition of bone formation by activating the Wnt/β-catenin signaling pathway *in vivo* and *in vitro*. *Sci. Rep.* **6,** 23827
30. Liang, W., Lin, M., Li, X., Li, C., Gao, B., Gan, H., Yang, Z., Lin, X., Liao, L., and Yang, M. (2012) Icariin promotes bone formation via the BMP-2/Smad4 signal transduction pathway in the hFOB 1.19 human osteoblastic cell line. *Int. J. Mol. Med.* **30,** 889–895
31. Zhai, Y. K., Guo, X. Y., Ge, B. F., Zhen, P., Ma, X. N., Zhou, J., Ma, H. P., Xian, C. J., and Chen, K. M. (2014) Icariin stimulates the osteogenic differentiation of rat bone marrow stromal cells via activating the PI3K-AKT-eNOS-NO-cGMP-PKG. *Bone* **66,** 189–198
32. Zhang, D., Fong, C., Jia, Z., Cui, L., Yao, X., and Yang, M. (2016) Icariin stimulates differentiation and suppresses adipocytic transdifferentiation of primary osteoblasts through estrogen receptor-mediated pathway. *Calcif. Tissue Int.* **99,** 187–198
33. García-Morales, V., Luaces-Regueira, M., and Campos-Toimil, M. (2017) The cAMP effectors PKA and Epac activate endothelial NO synthase through PI3K/Akt pathway in human endothelial cells. *Biochem. Pharmacol.* **2952,** 30567–30568
34. Suzuki, A., Ozono, K., Kubota, T., Kondou, H., Tachikawa, K., and Michigami, T. (2008) PTH/cAMP/PKA signaling facilitates canonical Wnt signaling via inactivation of glycogen synthase kinase-3β in osteoblastic Saos-2 cells. *J. Cell. Biochem.* **104,** 304–317
35. Labour, M. N., Riffault, M., Christensen, S. T., and Hoey, D. A. (2016) TGFβ1-induced recruitment of human bone mesenchymal stem cells is mediated by the primary cilium in a SMAD3-dependent manner. *Sci. Rep.* **6,** 35542
36. Bodle, J. C., Rubenstein, C. D., Phillips, M. E., Bernacki, S. H., Qi, J., Banes, A. J., and Loboa, E. G. (2013) Primary cilia: the chemical antenna regulating human adipose-derived stem cell osteogenesis. *PloS One* **8,** e62554
37. Ma, X. N., Ma, C. X., Shi, W. G., Zhou, J., Ma, H. P., Gao, Y. H., Xian, C. J., and Chen, K. M. (2017) Primary cilium is required for the stimulating effect of icaritin on osteogenic differentiation and mineralization of osteoblasts *in vitro*. *J. Endocrinol. Invest.* **40,** 357–366
38. Besschetnova, T. Y., Kolpakova-Hart, E., Guan, Y., Zhou, J., Olsen, B. R., and Shah, J. V. (2010) Identification of signaling pathways regulating primary cilium length and flow-mediated adaptation. *Curr. Biol.* **20,** 182–187
39. Raychowdhury, M. K., Ramos, A. J., Zhang, P., McLaughin, M., Dai, X. Q., Chen, X. Z., Montalbetti, N., Del Rocio Cantero, M., Ausiello, D. A., and Cantiello, H. F. (2009) Vasopressin receptor-mediated functional signaling pathway in primary cilia of renal epithelial cells. *Am. J. Physiol. Renal Physiol.* **296,** F87–F97
40. Willoughby, D., Wachten, S., Masada, N., and Cooper, D. M. (2010) Direct demonstration of discrete Ca^{2+} microdomains associated with different isoforms of adenylyl cyclase. *J. Cell Sci.* **123,** 107–117
41. Schmid, A., Meili, D., and Salathe, M. (2014) Soluble adenylyl cyclase in health and disease. *Biochim. Biophys. Acta* **1842,** 2584–2592
42. Litvin, T. N., Kamenetsky, M., Zarifyan, A., Buck, J., and Levin, L. R. (2003) Kinetic properties of "soluble" adenylyl cyclase: synergism between calcium and bicarbonate. *J. Biol. Chem.* **278,** 15922–15926
43. Chaloupka, J. A., Bullock, S. A., Iourgenko, V., Levin, L. R., and Buck, J. (2006) Autoinhibitory regulation of soluble adenylyl cyclase. *Mol. Reprod. Dev.* **73,** 361–368
44. Piggott, L. A., Bauman, A. L., Scott, J. D., and Dessauer, C. W. (2008) The A-kinase anchoring protein Yotiao binds and regulates adenylyl cyclase in brain. *Proc. Natl. Acad. Sci. U.S.A.* **105,** 13835–13840
45. Geng, W., Hill, K., Zerwekh, J. E., Kohler, T., Müller, R., and Moe, O. W. (2009) Inhibition of osteoclast formation and function by bicarbonate: role of soluble adenylyl cyclase. *J. Cell. Physiol.* **220,** 332–340
46. Reed, B. Y., Gitomer, W. L., Heller, H. J., Hsu, M. C., Lemke, M., Padalino, P., and Pak, C. Y. (2002) Identification and characterization of a gene with

base substitutions associated with the absorptive hypercalciuria phenotype and low spinal bone density. *J. Clin. Endocrinol. Metab.* **87,** 1476–1485

47. Ichikawa, S., Koller, D. L., Curry, L. R., Lai, D., Xuei, X., Edenberg, H. J., Hui, S. L., Peacock, M., Foroud, T., and Econs, M. J. (2009) Association of adenylate cyclase 10 (ADCY10) polymorphisms and bone mineral density in healthy adults. *Calcif. Tissue Int.* **84,** 97–102
48. Xie, Y. F., Shi, W. G., Zhou, J., Gao, Y. H., Li, S. F., Fang, Q. Q., Wang, M. G., Ma, H. P., Wang, J. F., Xian, C. J., and Chen, K. M. (2016) Pulsed electromagnetic fields stimulate osteogenic differentiation and maturation of osteoblasts by upregulating the expression of BMPRII localized at the base of primary cilium. *Bone* **93,** 22–32
49. Haslam, R. J., Davidson, M. M., and Desjardins, J. V. (1978) Inhibition of adenylate cyclase by adenosine analogues in preparations of broken and intact human platelets: evidence for the unidirectional control of platelet function by cyclic AMP. *Biochem. J.* **176,** 83–95
50. Park, Y. G., Kang, S. K., Noh, S. H., Park, K. K., Chang, Y. C., Lee, Y. C., and Kim, C. H. (2004) PGE2 induces IL-1β gene expression in mouse osteoblasts through a cAMP-PKA signaling pathway. *Int. Immunopharmacol.* **4,** 779–789
51. Pazour, G. J., Dickert, B. L., Vucica, Y., Seeley, E. S., Rosenbaum, J. L., Witman, G. B., and Cole, D. G. (2000) *Chlamydomonas* IFT88 and its mouse homologue, polycystic kidney disease gene tg737, are required for assembly of cilia and flagella. *J. Cell Biol.* **151,** 709–718
52. Clement, C. A., Larsen, L. A., and Christensen, S. T. (2009) Using nucleofection of siRNA constructs for knockdown of primary cilia in P19.CL6 cancer stem cell differentiation into cardiomyocytes. *Methods Cell Biol.* **94,** 181–197